Current Biology 19, 1255–1263, August 11, 2009 ©2009 Elsevier Ltd All rights reserved DOI 10.1016/j.cub.2009.06.038

Article

ITCH K63-Ubiquitinates the NOD2 Binding Protein, RIP2, to Influence Inflammatory Signaling Pathways

MingFang Tao,[1] Peter C. Scacheri,[2] Jill M. Marinis,[1] Edward W. Harhaj,[3] Lydia E. Matesic,[4] and Derek W. Abbott[1,*]
[1]Department of Pathology
[2]Department of Genetics
Case Western Reserve University School of Medicine, Cleveland, OH 44106, USA
[3]Department of Microbiology and Immunology, Sylvester Comprehensive Cancer Center, Miller School of Medicine, The University of Miami, Miami, FL 33136, USA
[4]Department of Biological Sciences, University of South Carolina, Columbia, SC 29208, USA

Summary

Background: The inability to coordinate the signaling pathways that lead to proper cytokine responses characterizes the pathogenesis of inflammatory diseases such as Crohn's disease. The Crohn's disease susceptibility protein, NOD2, helps coordinate cytokine responses upon intracellular exposure to bacteria, and this signal coordination by NOD2 is accomplished, in part, through K63-linked polyubiquitin chains that create binding surfaces for the scaffolding of signaling complexes.
Results: In this work, we show that the NOD2 signaling partner, RIP2, is directly K63-polyubiquitinated by ITCH, an E3 ubiquitin ligase that when lost genetically causes widespread inflammatory disease at mucosal surfaces. We show that ITCH is responsible for RIP2 polyubiquitination in response to infection with *listeria monocytogenes*. We also show that NOD2 can bind polyubiquitinated RIP2 and that whereas ITCH E3 ligase activity is required for optimal NOD2:RIP2-induced p38 and JNK activation, ITCH inhibits NOD2:RIP2-induced nuclear factor kappa B (NFκB) activation. This effect can be seen independently at the whole-genome level by microarray analysis of muramyl dipeptide (MDP)-treated *Itch*$^{-/-}$ primary macrophages.
Conclusions: These findings suggest that ITCH helps regulate NOD2-dependent signal transduction pathways and, as such, may be involved in the pathogenesis of NOD2-mediated inflammatory disease.

Introduction

The Crohn's Disease susceptibility protein, NOD2, is activated by intracellular exposure to both gram-positive and gram-negative bacteria [1–3]. Upon activation, it synergizes with toll-like receptors (TLRs) [1] to help generate a cytokine response that is carefully measured for precise delivery of the correct cytokines, the correct amount of those cytokines, and the correct duration of release of those cytokines [1–3]. Loss-of-function, Crohn's Disease-associated NOD2 alleles lose this ability and cause genetic Crohn's Disease [1–3], whereas gain-of-function NOD2 alleles cause the granulomatous disease Blau syndrome and a subset of sporadic early-onset sarcoidosis (EOS) cases [4, 5]. The perturbation of NOD2 signaling in diverse inflammatory diseases suggests that the coordination of inflammatory signaling pathways by NOD2 is critical and highly regulated.

Upon activation, NOD2 forms a complex with RIP2 [6–8]. RIP2 is an obligate component for NOD2 signaling; RIP2-knockout mice cannot generate nuclear factor kappa B (NFκB), p38, or JNK activation in response to the NOD2 agonist muramyl dipeptide (MDP, a breakdown product of bacterial peptidoglycan) [9–11]. Upon activation, the NOD2:RIP2 complex causes lysine-63 (K63) polyubiquitination of lysine-285 on NEMO [7, 8], a component of the NFκB signaling pathway that is necessary for NFκB activation [12]. Although evolving, current NOD2:RIP2 signaling models imply that this polyubiquitination of NEMO is responsible for binding to the TAK1 complex, allowing TAK1 to phosphorylate and activate I kappa kinase (IKK), thereby generating an NFκB response [8, 13–16]. Recently, work from independent labs has shown that RIP2 is also K63-polyubiquitinated in response to the in vitro agonist MDP and in response to intracellular bacterial infection [14, 15]. This polyubiquitination occurs on lysine-209 (K209) of RIP2 and is essential for NOD2:RIP2-induced NFκB activation [15]. Although one study presented data suggesting that TRAF6 might be mediating RIP2 polyubiquitnation [14], RIP2 polyubiquitination in TRAF6-deficient mouse embryonic fibroblasts (MEFs) was similar to that seen in wild-type (WT) MEFs [15], and although NOD2 activation can cause autoubiquitination and activation of TRAF6 [8], TRAF6 inhibition by either dominant-negative constructs or siRNA has no effect on NFκB activation by the NODs or RIP2 [8, 10]. Given these disparate findings, the E3 ligase(s) mediating RIP2 polyubiquitination is/are unknown, and the role that these potential E3 ligases play in affecting not just NFκB activation but also p38 and JNK activation downstream of NOD2 activation is unknown.

Ubiquitination plays a key role not only in the NOD2:RIP2 signaling pathway but also in other innate immune and inflammatory pathways. The TLRs, the IL-1 receptor, and the TNF receptor all required lysine-63 (K63) polyubiquitination of signaling proteins for optimal cytokine release [16]. Whereas the more common lysine-48 (K48) polyubiquitin linkage targets a protein to the proteosome for degradation, K63 polyubiquitin linkages are thought to serve a scaffolding function for signaling proteins such that signaling pathways can be activated and cytokine release achieved [16].

In this work, we find that ITCH (AIP4), a HECT-domain containing E3 ubiquitin ligase [17–21], directly ubiquitinates RIP2 to allow differential NOD2:RIP2 signaling through p38, JNK, and NFκB. *Itch* was first identified as the gene underlying the *itchy* mouse phenotype [17, 18]. This mouse has a variety of inflammatory and autoimmune phenotypes [17–20]. Mucosal surfaces of these mice show varying degrees of inflammation, and, on a C57BL/6J background, the *itchy* mice die of pulmonary pneumonitis [17–20]. When *itchy* mice are crossed into a *Rag1*-deficient background, autoimmune-mediated death no longer occurs [21]. However, mild mucosal inflammation was present in the *itchy* animals lacking *Rag1*, indicating a putative role for this E3 ligase that is independent of the

*Correspondence: dwa4@case.edu

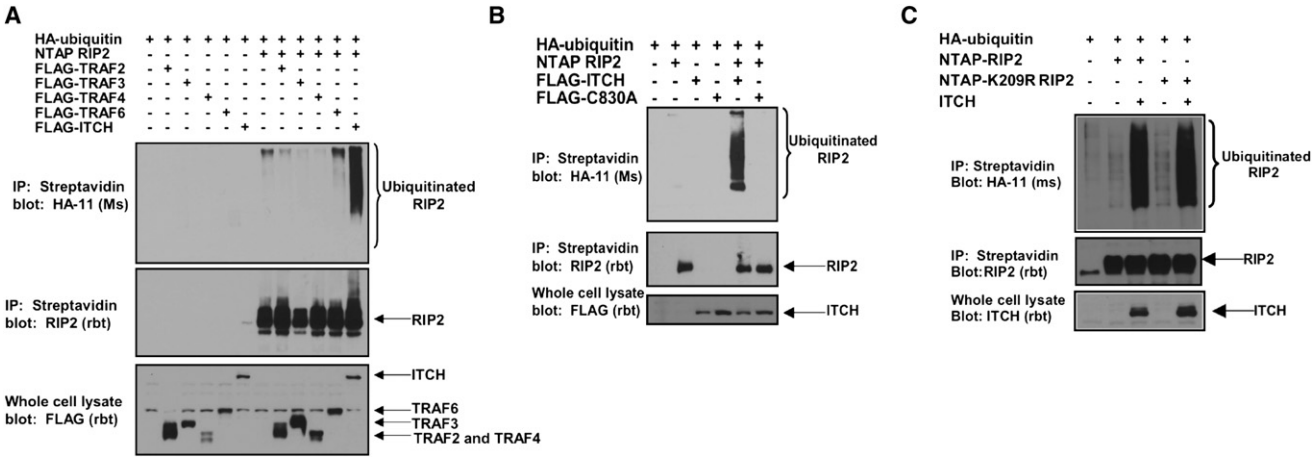

Figure 1. ITCH Expression Causes Ubiquitination of RIP2

(A) The E3 ligases TRAF2, TRAF3, TRAF4, TRAF6, and ITCH were transfected into HEK293 cells with HA-tagged ubiquitin and NTAP (streptavidin binding peptide)-tagged RIP2. After cell lysis, streptavidin precipitations were performed under high-stringency washing conditions (1 M NaCl, 1% SDS) to eliminate potential ubiquitinated RIP2 binding proteins. Immunoblotting was then performed. ITCH expression significantly increased RIP2 ubiquitination.

(B) NTAP-RIP2 was expressed in the presence of HA-ubiquitin and either WT ITCH or catalytically inactive C830A ITCH. The C830A ITCH mutant could not cause RIP2 ubiquitination.

(C) For determining whether ITCH caused ubiquitination of a previously published RIP2 ubiquitination site (lysine 209–K209), this lysine was mutated conservatively to arginine (K209R). After transfection and high-stringency washing of the streptavidin-agarose precipitate, immunoblotting was performed. ITCH caused indistinguishable ubiquitination of both WT and K209R RIP2, indicating that ITCH caused ubiquitination of separate site(s) on RIP2.

adaptive immune system and is instead important in the innate immune response [21]. By linking ITCH to the NOD2:RIP2 signaling pathway, this manuscript provides a potential mechanism for ITCH's role in the innate immune system.

Results

For the identification of E3 ligases that can polyubiquitinate RIP2, a panel of E3 ligases known to be involved in innate immunity and inflammation were screened for their ability to induce RIP2 polyubiquitination. TRAF2 (an E3 ligase activated by TNF [22]), TRAF3 (an E3 ligase activated by innate immune signals [23, 24]), TRAF4 (an E3 ligase that downregulates TLR signaling [25]), TRAF6 (an E3 ligase known to be activated by TLR and NOD signals [14]), and ITCH (a ubiquitously expressed E3 ligase, which mediates inflammatory signaling and T cell activation [18–21]) were transfected into 293 cells with HA-tagged ubiquitin and NTAP (streptavidin binding peptide)-tagged RIP2. All of the E3 ligases transfected were capable of autoubiquitination (Figure S1B, available online), suggesting that they were active in this system. After transfection, lysates were generated, and RIP2 was purified under stringent washing conditions (1 M NaCl, 1% SDS) through the use of streptavidin-agarose beads. Immunoblotting showed that ITCH expression caused strong RIP2 polyubiquitination and that none of the TRAFs tested significantly increased RIP2 polyubiquitination (Figure 1A, ubiquitin blot in Figure S1A; note that all ubiquitin expression blots are shown in the Supplemental Data [Figures S1, S3, S4, and S6]). To show that the RIP2 polyubiquitination was due to ITCH's E3 ligase activity, the catalytic cysteine in the HECT domain of ITCH was mutated to an alanine (C830A ITCH). When this catalytically inactive ITCH was expressed with RIP2, RIP2 polyubiquitination was lost (Figure 1B) and another HECT domain containing E3 ligase (E6AP) did not cause such increased RIP2 ubiquitination (Figure S2), suggesting that the catalytic activity of ITCH was necessary for RIP2 polyubiquitination and that this process was specific to ITCH. To then determine whether ITCH was the E3 ubiquitin ligase causing K209 ubiquitination, K209 on RIP2 was conservatively mutated to an arginine (K209R). Despite this mutation, ITCH-mediated polyubiquitination of RIP2 was unchanged in comparison to WT RIP2 (Figure 1C). Additional experiments showed only a small role for TRAF6 in ITCH-induced RIP2 ubiquitination. ITCH did not appreciably increase TRAF6 ubiquitination (Figure 2A). NOD2 coexpression with TRAF6 did not increase RIP2 polyubiquitination (Figure 2B). Inhibition of TRAF6 expression had a minimal effect on ITCH-induced RIP2 ubiquitination (Figure 2C), and inhibition of the E2 mediating TRAF6 activity (Ubc13) did not affect ITCH-induced RIP2 ubiquitination (Figure 2D). The fact that ITCH causes ubiquitination of a site distinct from K209 and that the TRAF6-Ubc13 axis plays a minimal role suggests that the ITCH mediation of RIP2 ubiquitination site(s) may be causing distinct signaling effects within the cell.

ITCH-induced RIP2 polyubiquitation could be direct or could occur through an intermediary E3 ligase. Initial mapping experiments showed that the CARD domain of RIP2 was required for ITCH-induced ubiquitination (Figure S3A). We have found that truncation of the CARD domain is essential for recombinant RIP2 expression in recombinant systems, so we utilized 293 cell-expressed, purified full-length NTAP-RIP2 for in vitro ubiquitination assays. For these assays, ITCH and the catalytically inactive (C830A ITCH) ITCH mutant were expressed as GST-fusion proteins in bacteria (Figure S3B). To determine the optimal E2 for the reaction, we incubated ITCH with E1, ATP, NTAP-RIP2, and a panel of E2s in standard in vitro ubiquitination assays. In the presence of UbcH5, UbcH6, and UbcH7, ITCH could directly ubiquitinate RIP2 (Figure S3C). After obtaining this information, we performed an in vitro ubiquitination assay to show that there was not a copurifying bacterial E3 ligase in the recombinant ITCH preparation. No RIP2 polyubiquitination was identified in the presence of C830A ITCH (Figure 3A), indicating that ITCH could directly ubiqutinate RIP2.

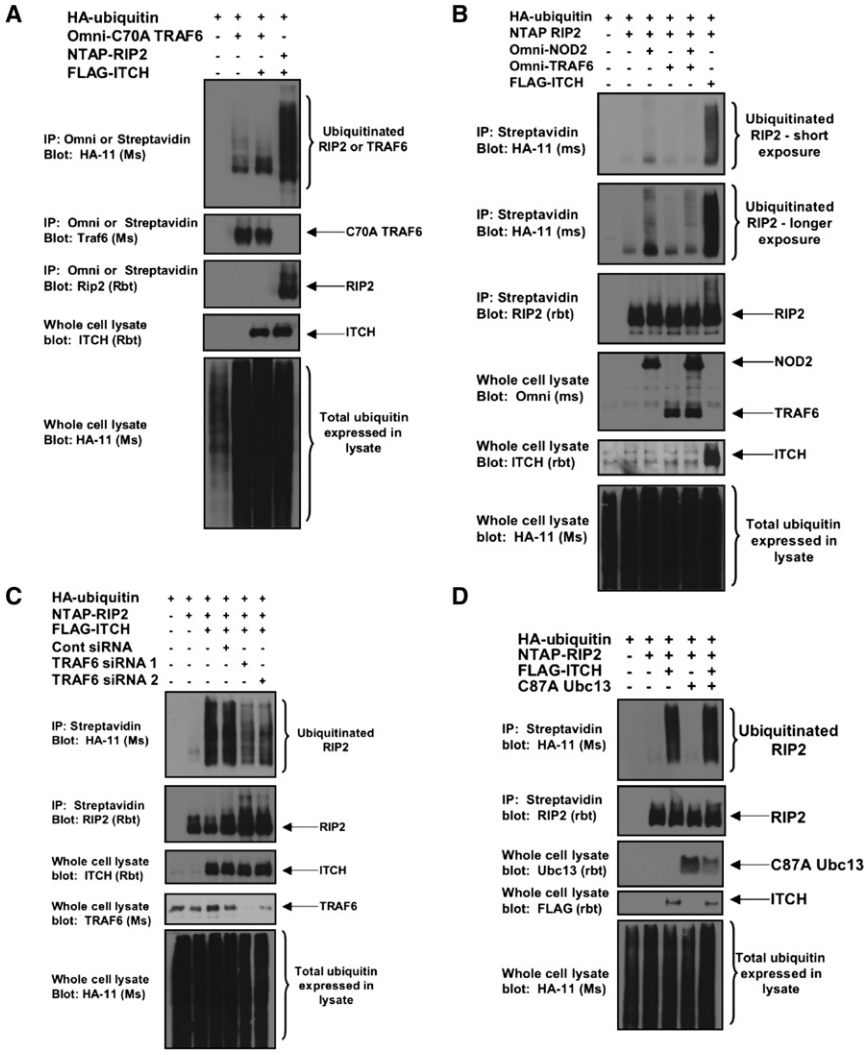

Figure 2. TRAF6/Ubc13 Has Minimal Involvement in ITCH-Induced RIP2 Ubiquitination

(A) For determining whether ITCH could ubiquitinate TRAF6, RING domain mutant TRAF6 (C70A) was transfected into 293 cells with ITCH. After immunoprecipitation in high-stringency buffer, immunoblotting was performed. Overexposing the blot revealed very little (if any) effect of ITCH on TRAF6 ubiquitination.

(B) For determining the strength of TRAF6-induced ubiquitination of RIP2 relative to ITCH-induced ubiquitiantion of RIP2, 293 cells were transfected with the indicated constructs. NOD2 was included, because a prior report had suggested that TRAF6 required NOD2 to ubiquitinate RIP2 [14]. After precipitation of RIP2 in high-stringency buffer, immunoblotting showed minimal ubiquitination of RIP2 relative to the cells transfected with ITCH.

(C) For determining whether TRAF6 affected ITCH-induced RIP2 ubiquitination, TRAF6 expression was inhibited by two separate siRNAs [8]. Inhibition of TRAF6 expression caused a small decrease in ITCH-induced RIP2 ubiquitination; however, the amount of remaining RIP2 ubiquitination was still high.

(D) For further determining the effect of TRAF6 on ITCH-induced RIP2 ubiquitination, the dominant-negative Ubc13 (C87A) was utilized. Expression of C87A Ubc13 had minimal effect on ITCH-induced RIP2 ubiquitination.

The lysine linkage on the ubiquitin itself influences the fate of the polyubiquitinated protein. ITCH has previously been shown to help synthesize K29-linked [26], K48-linked [19], and K63-linked [27] polyubiquitin chains. RIP2's in linkage was determined in three ways. First, in vitro ubiquitination assays were performed with the use of recombinant, purified ubiquitin molecules with specific lysine mutations. In these mutant ubiquitins, one lysine was mutated to an arginine while the other lysines remained intact. For instance, K6R ubiquitin contains a lysine mutated to an arginine at position 6, but all the other lysines on that mutant are intact. After in vitro ubiquitination reactions were performed, RIP2 was purified in high-stringency wash conditions and immunoblotting was performed. Whereas ubiquitin mutants containing lysines mutated to arginines at positions 6, 11, 29, and 48 could all form polyubiquitin chains on RIP2 that were indistinguishable from WT ubiquitin, K63R ubiquitin could not form these chains (Figure 3B), indicating that K63-linked polyubiquitin chains are formed on RIP2 by ITCH in vitro. As a second independent test for determining the ubiquitin linkage, a ubiquitin construct containing lysine only at position 48 (K48-only) or one containing lysine only at position 63 (K63-only) was transfected into 293 cells with NTAP-RIP2 and ITCH. After RIP2 was purified from the lysate, immunoblotting showed that only the K63-only ubiquitin allowed ITCH-mediated RIP2 polyubiquitination (Figure 3C), indicating again that ITCH induced K63-linked polyubiquitin-chain formation on RIP2. As a last independent test of the ubiquitin linkage, we utilized a deubiquitinase, A20, that recognizes specific proteins with K63-polyubiquitinated chains and deubiquitinates those proteins [28, 29]. Given that A20 downregulates the NOD2:RIP2 signaling pathway [29, 30] and has been shown to deubiquitinate K63-linkages on RIP2 [29], we reasoned that if RIP2 was K63-polyubiquinated by ITCH, then A20 should recognize the K63-linked chains and remove them. To this end, A20 was expressed with RIP2 and ITCH. A20 expression caused a significant decrease in the amount of ITCH-induced polyubiquitinated RIP2 (Figure 3D), further suggesting that ITCH caused K63-linked polyubiquitination of RIP2. Thus, three separate experimental methods suggest that ITCH polyubiquitinates RIP2 through K63-specific linkages.

Because ITCH-induced K63-linked polyubiquitination of RIP2 may affect NOD2:RIP2-induced signaling pathways, we wanted to determine whether RIP2 polyubiquitination affected NOD2 binding and whether NOD2 could bind to polyubiquitinated RIP2. For this reason, Omni-tagged NOD2 was expressed with RIP2 with either ITCH or catalytically inactive C830A ITCH. NOD2 was immunoprecipitated. Immunoblotting showed that NOD2 could bind to RIP2 in the presence of ITCH or C830A ITCH. However, when ITCH was present, there was not only a significant shift in the mobility of total RIP2 (Figure 4A, second panel from bottom) but also a significant shift in the mobility of the RIP2 that was bound to NOD2 (Figure 4A, top panel). This shift in the RIP2 bound to NOD2

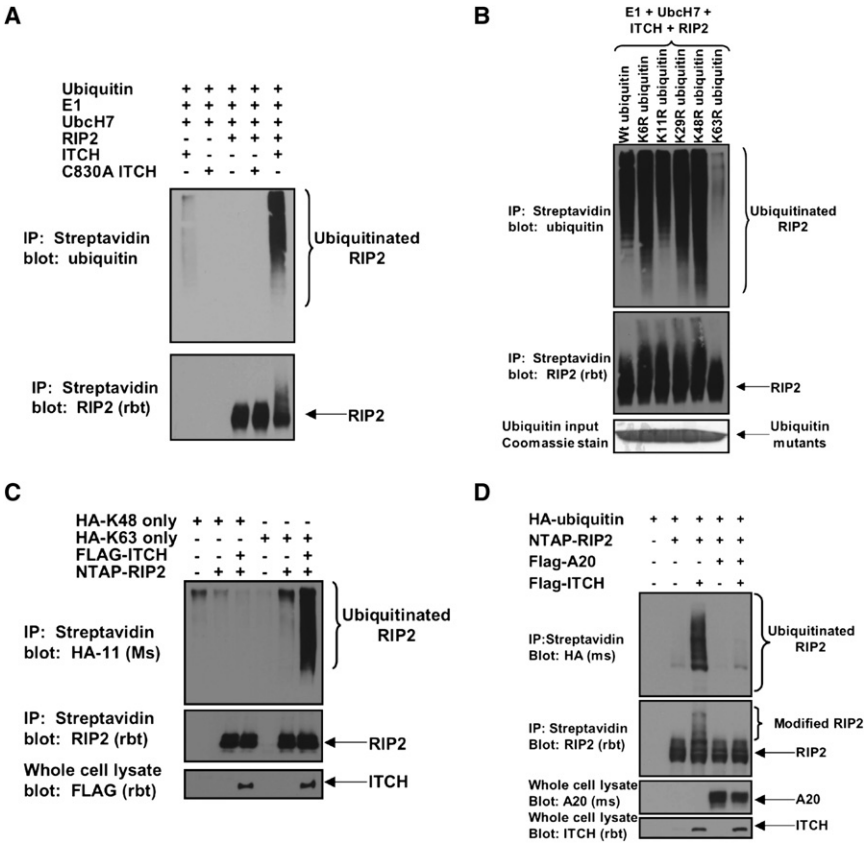

Figure 3. ITCH Ubiquitinates RIP2 Directly by Using K63 Ubiquitin Linkages

(A) NTAP-RIP2 was purified from transfected HEK293 cells and incubated with recombinant ITCH, UbcH7, ATP, ubiquitin, and E1 for 60 min at 37°C. RIP2 was then repurified, and immunoblots were performed. ITCH could directly ubiquitinate RIP2, and the catalytically inactive C830A ITCH lost this ability.

(B) In vitro ubiquitination reactions were performed with the use of ubiquitin mutants specifically mutated at the indicated lysine. RIP2 was then repurified, and immunoblotting was performed. Only K63R ubiquitin caused a significant decxrease in RIP2 polyubiquitination.

(C) 293 cells were transfected with RIP2, ITCH, and either HA-tagged K48-only ubiquitin or HA-tagged K63-only ubiquitin (all other lysines, except K48 and K63, respectively, were mutated to arginine). K63-only ubiquitin caused strong RIP2 polyubiquitination, whereas K48-only ubiquitin did not.

(D) For further demonstrating this K63 linkage, the K63 deubiquitinase A20 was transfected into 293 cells with RIP2, HA-ubiquitin, and/or ITCH. After precipitation of RIP2, immunoblotting showed that A20 expression could significantly impair RIP2 polyubiquitination.

was present only in cells expressing ITCH and not in cells expressing catalytically inactive C830A ITCH (Figure 4A, top panel). To further show that NOD2 can bind to polyubiquitinated RIP2, RIP2 was again expressed with HA-tagged ubiquitin, Omni-tagged NOD2, and a limited amount of ITCH. NOD2 was initially purified via the 6XHis component of the Omni-tag via nickel beads and then eluted in 200 mM Imidazole. This NOD2 isolate was then split into two fractions. The first fraction was subjected to streptavidin-agarose for isolation of the fraction of RIP2 bound to NOD2. The second fraction was subjected to anti-HA immunoprecipitation for isolation of the ubiquitinated proteins present in the NOD2 isolate. Within the NOD2 isolate, ubiquitinated RIP2 was present, as shown by the ability of the HA antibody to immunoprecipitate a significant amount of RIP2 (Figure 4B, second panel from top, lane 4) and by the ability of the streptavidin-agarose to precipitate a significant amount of ubiquitinated RIP2 (Figure 4B, upper panel, lane 3). These findings suggest that NOD2 can bind to polyubiquitinated RIP2.

We then sought to determine the effect of ITCH on NOD2:RIP2 signaling pathways. NOD2:RIP2 complex activation causes not only NFκB activation, but also activation of a number of signaling pathways, including JNK and p38 [11, 14, 31]. To determine ITCH's role in NOD2:RIP2 signaling, we utilized four individual siRNAs to inhibit ITCH's expression. Inhibition of ITCH expression by these siRNAs has limited effect on the activation of JNK, IKKβ, or p38 by overexpression of downstream MAP3Ks (Figures S5A–S5D). Each siRNA targeting ITCH (and a control siRNA) was transfected with RIP2 and with FLAG-JNK (Figure 5A), HA-IKKβ (Figure 5B), or FLAG-p38 (Figure 5C). Immunoprecipitations were then performed for the isolation of JNK, IKKβ, or p38. Immunoblotting showed that in these cells in which the individual siRNAs were transfected, ITCH expression was significantly reduced (Figures 5A, 5B, and 5C, bottom panel). Loss of ITCH expression caused significant decreases in both JNK (Figure 5A) and p38 (Figure 5C) activity. In contrast, loss of ITCH expression enhanced RIP2-induced IKKβ activation (Figure 5B). For further independent validation of this finding, catalytically inactive C830A ITCH was used. In these conditions, C830A ITCH can act in a dominant-negative manner ([19], Figure S6A) and has limited effect on activation of JNK, IKKβ, or p38 by overexpression of downstream MAP3Ks (Figures S6B–S6D). Dominant-negative C830A ITCH did, however, cause loss of RIP2-induced activation of both JNK and p38 (Figures S6B and S6C). Consistent with published results on the role of ITCH in negatively regulating TNF-induced NFκB signaling [21], ITCH expression caused a strong decrease in RIP2-induced IKKβ activation, whereas expression of C830A ITCH not only reversed this inhibition but also enhanced RIP2-induced IKKβ activation (Figure S6B).

Because these experiments utilized overexpression and in vitro ubiquitination assays, we attempted to determine whether loss of ITCH expression could affect RIP2 polyubiquitination in more endogenous systems. RIP2 is an essential component of cellular NFκB and MAP kinase signaling pathways initiated by cellular infection by the gram-positive intracellular pathogen, *Listeria monocytogenes* [11, 31–33]. *Listeria monocytogenes* enters the body by infecting the gastrointestinal epithelium. For this reason, we utilized the gastrointestinal epithelial cell line, HT-29, which expresses NOD2 [34] to determine whether loss of ITCH expression affected RIP2 polyubiquitination in response to intracellular *Listeria* infection. After transfection with the ITCH-targeting siRNAs, HT-29 cells were infected with *Listeria monocytogenes* at a multiplicity of infection (MOI) of 3:1. Endogenous RIP2 was then immunoprecipitated. Under these conditions, ITCH expression was

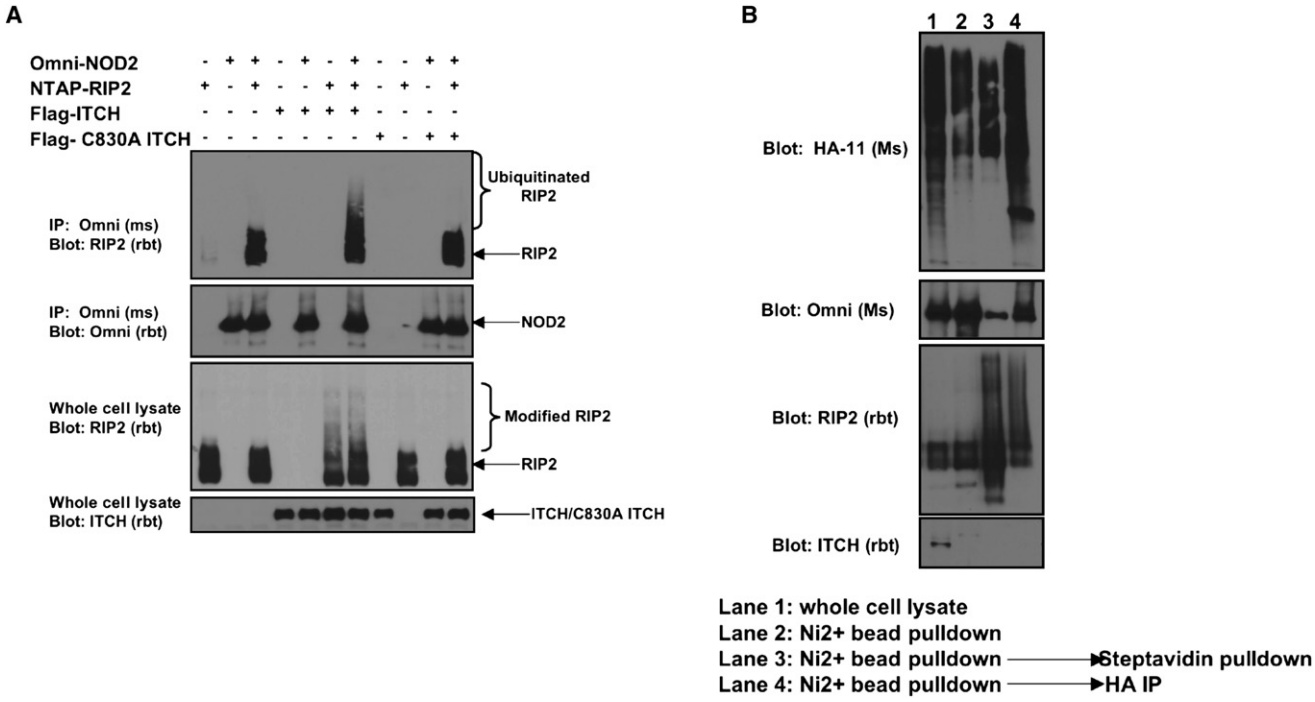

Figure 4. NOD2 Binds to Ubiquitinated RIP2

(A) Omni-tagged NOD2 was expressed in 293 cells with RIP2 and either WT ITCH or catalytically inactive C830A ITCH. NOD2 was immunoprecipitated via its Omni tag, and immunoblots were performed. RIP2 polyubiquitination was enhanced in the presence of ITCH and NOD2 (whole-cell lysate anti-RIP2 panel). These modified forms of RIP2 were present in the NOD2 immunoprecipitates (upper panel). These modified forms were not seen in the presence of catalytically inactive C830A ITCH; however, binding of RIP2 to NOD2 was unchanged.

(B) Omni-tagged NOD2 was expressed with RIP2, HA-tagged ubiquitin, and ITCH. Ni^{2+} beads were used for isolating NOD2 via the 6XHis component of the Omni tag, and NOD2 was then released from the beads by 200 mM Imidazole. This elution was then split into two fractions. One fraction was immunoprecipitated with an anti-HA antibody for isolation of ubiquitinated proteins present in NOD2 isolates, and the second fraction was subjected to streptavidin-agarose pulldowns for isolation of RIP2 from the NOD2 isolate. The HA-ubiquitin immunpreciptates from the NOD2 isolate contained RIP2 (RIP2 blot, lane 4), and RIP2 precipitates from the NOD2 isolate contained ubiquitinated RIP2 (HA blot, lane 3).

significantly inhibited and RIP2 polyubiquitination was attenuated in cells in which ITCH expression was inhibited (Figure 6A). To determine the signaling effects of *listerial* infection of HT-29 s in which ITCH expression was inhibited, HT-29 cells were infected with *listeria* under the conditions described above. Forty-five minutes after extensive washing with PBS and the subsequent addition of gentamycin to serum-free media, killing any remaining extracellular bacteria, lysates were generated, and immunoblotting was performed. Activity of JNK and p38 was attenuated in cells in which ITCH expression was inhibited. In contrast, NFκB activity (as shown by total IκBα and phospho-IκBα) was increased relative to the control siRNA-transfected cells (Figure 6B). Because listeria monocytogenes contains numerous PAMPs that will activate additional innate immune signaling pathways, a partial response is not surprising. In all, though, the inhibition of RIP2

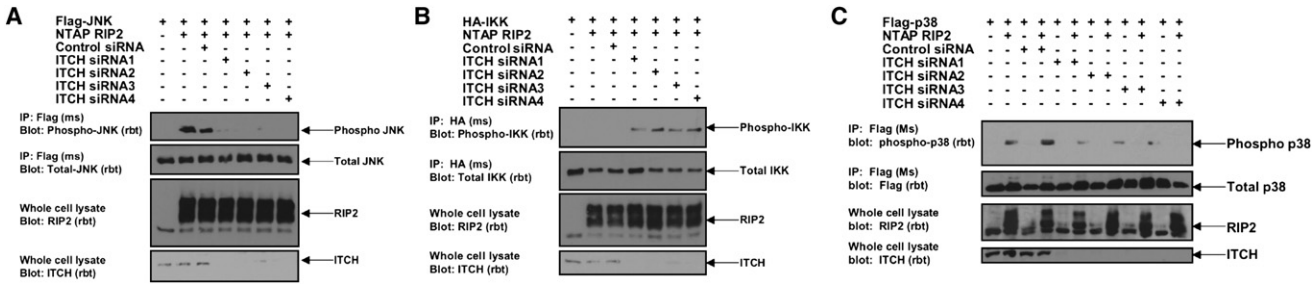

Figure 5. Inhibition of ITCH Expression Enhances NFκB Signaling and Decreases p38 and JNK Activation

(A) HEK293 cells were transfected with FLAG-JNK (0.5 μg), RIP2 (1 μg), and either a control siRNA or siRNAs targeting ITCH. JNK was purified via its FLAG tag, and immunoblotting was performed. Decreased ITCH expression strongly inhibited RIP2-induced JNK activation.

(B) HEK293 cells were transfected with HA-IKKβ (0.5 μg), RIP2 (0.5 μg), and either a control siRNA or siRNAs targeting ITCH. IKKβ was immunopurified via its HA tag, and immunoblotting was performed. Decrease in ITCH expression caused increased IKKβ activation.

(C) HEK293 cells were transfected with FLAG-p38 (0.5 μg), RIP2 (2.5 μg), and either a control siRNA or siRNAs targeting ITCH. p38 was purified via its FLAG tag, and immunoblotting was performed. In the presence of RIP2, inhibition of ITCH expression attenuated p38 activity.

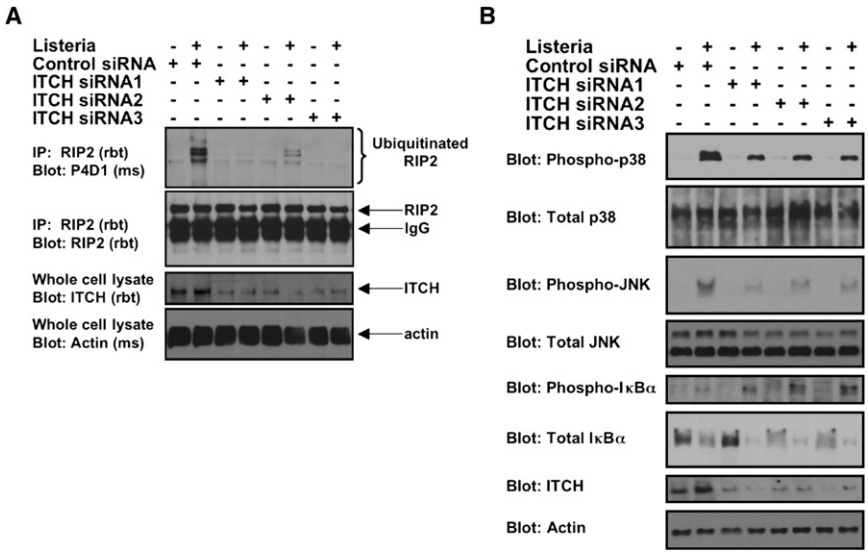

Figure 6. Inhibition of ITCH Expression Causes Decreased RIP2 Ubiquitination in Response to *Listeria* Infection

(A) HT29 cells were transfected with the siRNAs targeting ITCH or with a control siRNA. These cells were then infected with exponentially growing *Listeria monocytogenes* at an MOI of 3:1. Endogenous RIP2 was immunoprecipitated from the lysate, and immunoblotting was performed. RIP2 polyubiquitination was induced by *Listeria* infection, but this polyubiquitination was decreased when ITCH expression was inhibited.

(B) HT-29 cells in which ITCH expression was inhibited by siRNA transfection were infected with *Listeria*. Lysates were generated, and immunoblotting was performed. Inhibition of ITCH expression attenuated p38 and JNK activation but increased NFκB activity.

ubiquitination (Figure 6A), coupled with the signaling responses seen in Figure 6B, suggests that ITCH affects NOD2:RIP2 signaling.

For the study of the MDP-induced signaling alterations due to loss of ITCH expression in a genetic system, age (8-wk-old)- and sex-matched C57BL/6J WT and *itchy* mice were sacrificed, and their bone marrow was harvested to obtain bone-marrow-derived macrophages (BMDMs). After differentiation, these macrophages were treated with MDP for 60 min. RIP2 was then immunoprecipitated under stringent washing conditions. Immunoblotting showed that RIP2 was ubiquitinated in these cells upon MDP treatment but that this ubiquitination was very strongly attenuated in the *itchy* macrophages (Figure 7A). Signaling experiments were then performed. Macrophages from *itchy* mice had significantly lower levels of MDP-induced JNK and p38 activity and significantly higher levels of NFκB activity (as shown by increased degradation of IκBα and increased levels of phospho-IκBα [Figure 7B]). The *itchy* cells did have increased basal phosphorylation of IκBα, indicating the possibility of increased basal NFκB activation. In all, these signaling experiments closely mirror the results found in both the 293 cell overexpression system and the HT-29 infection model.

Next, for the determination of whether ITCH was in the NOD2:RIP2 pathway, WT and Itch$^{-/-}$ macrophages were either left untreated or treated with 10 μg/mL for 16 hr. Total RNA was extracted and microarray analysis was performed. After baseline gene-expression differences between the WT and Itch$^{-/-}$ macrophages were subtracted out, whole-genome clustering analysis showed that WT macrophages could be distinguished from Itch$^{-/-}$ macrophages upon MDP treatment (Figure 7C). This experiment was performed in duplicate, and both results are shown. The data were then analyzed for the inducible expression of known NFκB target genes. Itch$^{-/-}$ macrophages had significantly higher expression of NFκB target genes, including *BCL2*, *CCL3*, *IL-1*, *TNF*, *ICAM*, and *TNFAIP2* (Figure 7D). These microarray analyses show that Itch$^{-/-}$ cells have a different genetic response to MDP stimulation and that a number of NFκB target genes are upregulated. These results, when coupled with the biochemistry/molecular biology of Figures 1–5, the siRNA results of Figure 6, and the signaling differences between WT and Itch$^{-/-}$ macrophages illustrated in Figures 7A and 7B, strongly suggest that ITCH-mediated RIP2 ubiquitination has functional consequences.

Conclusions

The work presented in this manuscript suggests that ITCH directly ubiquitinates RIP2 to specify NOD2 signaling responses. RIP2 has previously been shown by three independent groups to be K63-polyubiquitinated [14, 15, 35]. One group mapped the site of polyubiquitination on RIP2 to lysine-209 (K209) [15]. This K209 ubiquitination site is required for NOD2:RIP2-induced NFκB activation [15]. However, although this group found the ubiquitination to be independent of TRAF6 [15], another group presented data suggesting that TRAF6 was the E3 ligase [14]. For this reason, it is unclear whether K209 ubiquitination is mediated through the TRAF proteins and the E2 ligase Ubc13 [14, 15]. Our results, like those of the Nunez and Inohara labs, suggest TRAF6-independent ubiquitination machinery for NOD2:RIP2 signaling. Unlike the TRAF proteins, ITCH-induced RIP2 ubiquitination does not require Ubc13 (Figure 2D). Inhibition of TRAF6 expression showed only a small effect on ITCH-induced RIP2 ubiquitination (Figure 2C), and previous work from our lab [8] and Gabriel Nunez's lab [36] showed that although TRAF6 could be activated by NOD2, neither dominant-negative TRAF6 [36] nor siRNA inhibition of TRAF6 [8] had any bearing on NOD:RIP2-induced NFκB activation. Thus, these results, coupled with the findings in this manuscript, suggest that ITCH-induced RIP2 ubiquitination is not dependent on TRAF6. Additionally, a report published while this manuscript was in review also suggests that RIP2 ubiquitination is independent of TRAF6 [35]. The Saleh group found that the cIAP proteins could both K48 and K63 ubiquitinate RIP2 and that depending on the cell type, this ubiquitination was required for p38, JNK, and/or NFκB signaling [35]. Although our own unpublished findings indicate that cIAP-1 causes predominantly K48-linked polyubiquitination of RIP2, given the presence of at least 1000 E3 ubiquitin ligases in the genome, it is not surprising that multiple E3 ubiquitin ligases can act on a protein to exert signaling effects. Further work will be required to determine the interplay between the cIAPs and ITCH in NOD signaling pathways.

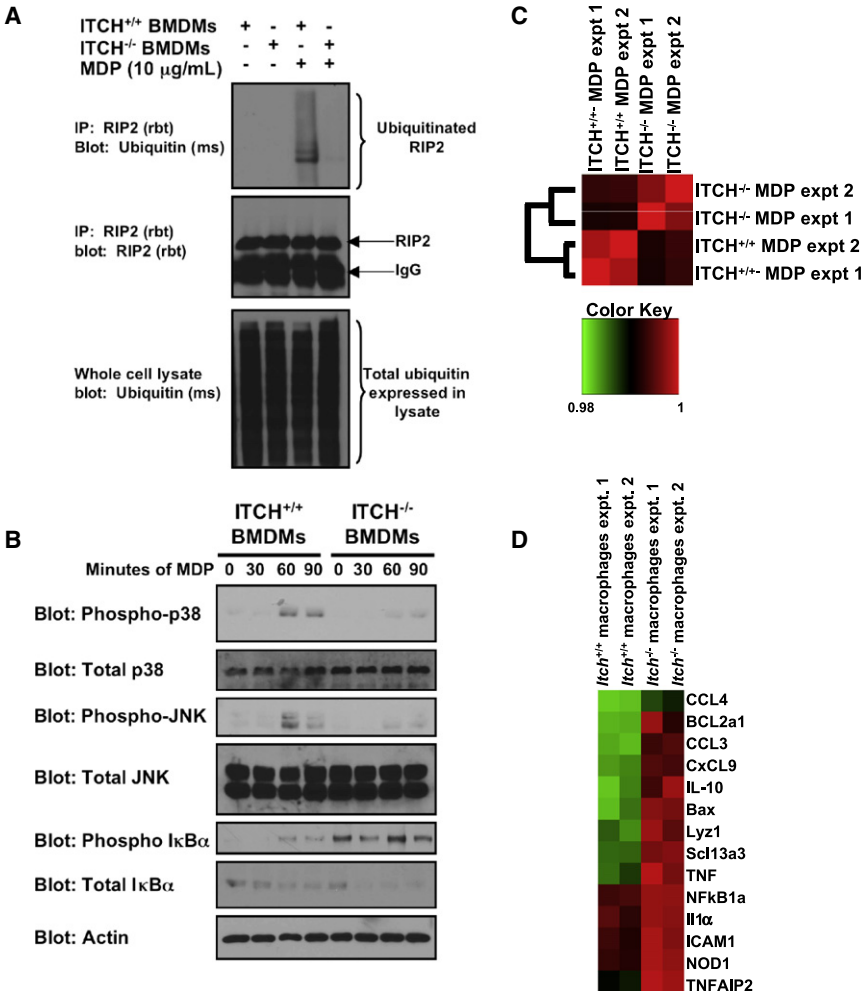

Figure 7. Loss of ITCH Expression Causes Increased NFκB-Driven Signaling Responses

(A) BMDMs from 8-wk-old, sex-matched, WT C57BL/6 or *itchy* (*Itch*$^{-/-}$) C57BL/6 mice were generated. These cells either were left untreated or were exposed to MDP (10 μg/mL) for 60 min. RIP2 was immunoprecipitated, and immunoblotting was performed. MDP-induced RIP2 ubiquitination was strongly attenuated in the *Itch*$^{-/-}$ macrophages.

(B) BMDMs from WT or *Itch*$^{-/-}$ mice were treated with MDP. Lysates were generated, and immunoblotting was performed with the indicated antibodies. ITCH$^{-/-}$ macrophages showed diminished p38 and JNK activity and increased NFκB activity.

(C) These BMDMs either were left untreated or were treated with 10 μg/mL MDP for 16 hr. Total RNA was harvested, and genomic gene expression was evaluated by microarray expression analysis. After subtracting out the basal changes between the macrophages in the untreated state, the MDP-treated WT macrophages could be blindly and bioinformatically distinguished from the MDP-treated *Itch*$^{-/-}$ macrophages.

(D) Analysis of the gene expression differences between the MDP-treated WT and *Itch*$^{-/-}$ macrophages showed increased expression of NFκB target genes.

ITCH itself plays a role in the immune system. While it is ubiquitously expressed, mice lacking *Itch* develop uncontrolled inflammatory responses at mucosal surfaces [17, 18, 21]. The lethal aspect of the phenotype is dependent on the adaptive immune response; *itchy* mice crossed onto a *Rag1*-deficient background show no death due to pulmonary pneumonitis. However, the inflammatory phenotype partially persists in these mice [21], suggesting that ITCH also has a role in regulating the innate immune response. The work described here suggests that ITCH may do this by modulating signaling downstream of NOD2:RIP2 activation. Synthesizing these data with previously published reports [6–8, 13–15, 30, 36], we hypothesize that upon cellular infection and MDP exposure, RIP2 dissociates from the protein kinase, MEKK4, to bind to NOD2. Upon binding to NOD2, a subset of RIP2 becomes ubiquitinated on K209 to stimulate NEMO ubiquitination and subsequent NFκB activation. Separately, a second subset of RIP2 is polyubiquitinated by ITCH to activate JNK and p38 signaling. We hypothesize that ITCH competes with the K209 E3 ligase to dictate whether JNK and p38 are or whether NFκB is the predominant downstream pathway after NOD2:RIP2 activation. It will be important to determine the ITCH-induced polyubiquitination site on RIP2 and to determine whether differential polyubiquitination between K209 and the ITCH-mediated site dictates signal specificity downstream of NOD2. It will also be important to determine whether the phenotype of the *itchy* mice is influenced by the NOD2 signaling pathway and whether loss of components of the NOD2 signaling pathway can complement the inflammatory phenotype seen in the *itchy* mice. Lastly, a key question remains: Where in the cell is NOD2:RIP2 signaling taking place? NOD2 can localize to the membrane upon exposure to MDP [37]. MDP uptake by macrophages appears to be due to an endocytic process involving pannexin-1, and MDP is ultimately delivered to and possibly escapes from the phagolysosome [38]. Because ITCH has been published to localize to endocytic compartments [19, 26], we suspect that, upon MDP uptake, the NOD2:RIP2 physiologic interaction with ITCH localizes to endocytic compartments and that ITCH helps regulate the initial signaling events after MDP uptake. In this light, an alternative explanation for the data presented in the manuscript is that ITCH ubiquitination causes preferential degradation of RIP2 to decrease NFκB activation. Despite these questions and the need for future studies, this work suggests an important regulatory role for ITCH in NOD2:RIP2 signaling pathways and suggests that ITCH may have a role in the pathophysiology of NOD2-driven inflammatory diseases.

Experimental Procedures

Cell Culture, Immunoprecipitations, and Immunoblotting

HEK293 and HT-29 (ATCC) cells were grown in DMEM containing 5% FBS. Transfections were performed by calcium phosphate precipitation as previously described [7]. Immunoprecipitations were performed in 50 mM Tris (pH 7.5), 150 mM NaCl, 1% Triton X-100, 1 mM EDTA, 1 mM EGTA, 1 mM β-glycerophosphate, 1 mM PMSF, 1 mM $NaVO_4$, and 10 nM Calyculin A in the presence of protease inhibitor cocktail (Sigma). After protein G sepharose beads were added, IPs were washed at least five times before immunoblotting was performed. For IP-ubiquitination assays, cells were lysed in

high-salt modified Cell Signaling Lysis Buffer containing 1 M NaCl and from 0.25% to 1% SDS, as indicated in the text. Immunoblotting was performed as previously described [7].

Antibodies, Plasmids, and Reagents

Myc (9E10), RIP2, actin, and Omni antibodies were obtained from Santa Cruz Technology. P4D1 (ubiquitin), Myc (rabbit), phospho IKKα/β, phospho-IκBα, IKKβ, IκBα, NEMO, phospho-JNK, JNK, phospho-p38, and total p38 antibodies were obtained from Cell Signaling Technology. NTAP-RIP2 was generated by subcloning the Omni-RIP2 construct (EcorI-XhoI) into the NTAP vector (Stratagene). Omni-RIP2, HA-ubiquitin, Myc-NEMO K399R, HA-RIP2, Omni-NOD2, FLAG-TAK1, FLAG-p38, HA-MEKK4, FLAG-JNK, ITCH, C830A ITCH, and HA-IKKβ were used as previously described [7, 8, 30, 36]. The K209R RIP2 construct was generated by Quickchange site-directed mutagenesis (Stratagene).

In Vitro Ubiquitination Assays

ITCH and C830A ITCH were subcloned into pGEX-4T vectors and purified via standard methodology. For the in vitro ubiquitination assays, E1, the indicated E2s, WT ubiquitin, and the indicated ubiquitin mutants were all obtained from Boston Biochem. Reaction mixtures consisted of a buffer containing 25 mM HEPES (pH 7.4), 100 mM NaCl, 1 mM DTT, 10 μM MG132, 1 μM ubiquitin aldehyde, 4 mM ATP, 50 ng/mL E1, 1 μg/mL ubiquitin, 200 ng/mL E2, 150 ng/mL ITCH, and NTAP-RIP2 purified from transfected HEK293 cells. Reactions were allowed to proceed at 37°C for 1 hr. The reactions were then diluted in 900 μl of Cell Signaling lysis buffer containing 1 M NaCl and 0.5% SDS, and RIP2 was then immunopurified from the in vitro reaction.

siRNA

Four separate siRNAs were purchased from QIAGEN. The sequences of these were as follows: siRNA1, CACGGGCGAGUUUACUAUGUA; siRNA2, CAAGAGCUAUGAGCAACUGAA; siRNA3, AUGGGUAGCCUCACCAUGAAA; siRNA4, UGCCGCCGACAAAUACAAAUA. HT-29 cells were transfected with Dharmafect 4 (Fisher) according to the manufacturer's protocol.

Listeria Infection

Listeria monocytogenes were grown overnight in BHI media at 37°C. The next morning, the *listeria* were diluted 1:10 and allowed to grow for another 45 min, such that they were in exponential growth phase. OD_{600}s were performed to quantitate the numbers of listeria and the exponential growth rate of that listerial culture. *Listeria* was added to HT-29 cells at a MOI of 3:1. Forty-five minutes after the addition of listeria to the HT-29 cells, fresh media containing Gentamycin Sulfate (50 μg/mL final concentration) was added to kill extracellular bacteria. The infection was then allowed to proceed for another hour before lysates were generated, protein concentrations were standardized, and RIP2 was immunoprecipitated. High-stringency washing and immunoblotting and signaling assays on lysates were performed as described above.

Microarray Gene Expression Analysis

Total RNA was isolated from WT and *Itch*$^{-/-}$ macrophages via a QIAGEN kit. Integrity was analyzed by agarose gel electrophoresis, and RNA quantities were standardized. Microarray analysis on the RNA was performed by the Cleveland Clinic Research Institute Core Facility with the use of Illumina Mouse-6 Bead Chips. Raw Illumina microarray data were quintile normalized, and significant genes ($p < 0.05$, adjusted for false discovery rate) were identified with the lumi package in R [39]. Hierarchical clustering and heatmap analysis of significant genes were performed with Cluster 3.0 and Java TreeView [40].

Supplemental Data

Supplemental Data include seven figures and can be found with this article online at http://www.cell.com/current-biology/supplemental/S0960-9822(09)01314-1.

Acknowledgments

This work was supported by grants R01GM86550-01 (D.W.A.), R21AI076886-01 (D.W.A.), and R01HD056369 (P.C.S.) from the National Institutes of Health and award 10061206.01 from the Burroughs Wellcome Career Awards in Biomedical Sciences (D.W.A.). We thank XiaoXia Li (CCF, Cleveland, OH, USA) for supplying the FLAG-tagged TRAF2, TRAF3, and TRAF4 constructs.

Received: March 21, 2009
Revised: June 15, 2009
Accepted: June 16, 2009
Published online: July 9, 2009

References

1. Inohara, N., Chamaillard, M., McDonald, C., and Nunez, G. (2005). NOD-LRR proteins: role in host-microbial interactions and inflammatory disease. Annu. Rev. Biochem. *74*, 355–383.
2. Fritz, J.H., Ferrero, R.L., Philpott, D.J., and Girardin, S.E. (2006). Nod-like proteins in immunity, inflammation and disease. Nat. Immunol. *7*, 1250–1257.
3. Strober, W., Murray, P.J., Kitani, A., and Watanabe, T. (2006). Signalling pathways and molecular interactions of NOD1 and NOD2. Nat. Rev. Immunol. *6*, 9–21.
4. Kanneganti, T.D., Lamkanfi, M., and Núñez, G. (2007). Intracellular NOD-like receptors in host defense and disease. Immunity *27*, 549–559.
5. Henckaerts, L., and Vermeire, S. (2007). NOD2/CARD15 disease associations other than Crohn's disease. Inflamm. Bowel Dis. *13*, 235–241.
6. Inohara, N., Koseki, T., Lin, J., del Peso, L., Lucas, P.C., Chen, F.F., Ogura, Y., and Núñez, G. (2000). An induced proximity model for NF-kappa B activation in the Nod1/RICK and RIP signaling pathways. J. Biol. Chem. *275*, 27823–27831.
7. Abbott, D.W., Wilkins, A., Asara, J.M., and Cantley, L.C. (2004). The Crohn's disease protein, NOD2, requires RIP2 in order to induce ubiquitinylation of a novel site on NEMO. Curr. Biol. *14*, 2217–2227.
8. Abbott, D.W., Yang, Y., Hutti, J.E., Madhavarapu, S., Kelliher, M.A., and Cantley, L.C. (2007). Coordinated Regulation of Toll-Like Receptor and NOD2 Signaling by K63-Linked Polyubiquitin Chains. Mol. Cell. Biol. *27*, 6012–6025.
9. Girardin, S.E., Boneca, I.G., Viala, J., Chamaillard, M., Labigne, A., Thomas, G., Philpott, D.J., and Sansonetti, P.J. (2003). Nod2 is a general sensor of peptidoglycan through muramyl dipeptide (MDP) detection. J. Biol. Chem. *278*, 8869–8872.
10. Inohara, N., et al. (2003). Host recognition of bacterial muramyl dipeptide mediated through NOD2. Implications for Crohn's disease. J. Biol. Chem. *278*, 5509–5512.
11. Park, J.H., Kim, Y.G., McDonald, C., Kanneganti, T.D., Hasegawa, M., Body-Malapel, M., Inohara, N., and Nunez, G. (2007). RICK/RIP2 mediates innate immune responses induced through Nod1 and Nod2 but not TLRs. J. Immunol. *178*, 2380–2386.
12. Hayden, M.S., and Ghosh, S. (2008). Shared principles in NF-kB signaling. Cell *132*, 344–362.
13. Windheim, M., Lang, C., Peggie, M., Plater, L.A., and Cohen, P. (2007). Molecular mechanisms involved in the regulation of cytokine production by muramyl dipeptide. Biochem. J. *404*, 179–190.
14. Yang, Y., Yin, C., Pandey, A., Abbott, D., Sassetti, C., and Kelliher, M.A. (2007). NOD2 pathway activation by MDP or Mycobacterium tuberculosis infection involves the stable polyubiquitination of Rip2. J. Biol. Chem. *282*, 36223–36229.
15. Hasegawa, M., Fujimoto, Y., Lucas, P.C., Nakano, H., Fukase, K., Núñez, G., and Inohara, N. (2007). A critical role of RICK/RIP2 polyubiquitination in Nod-induced NF-kappaB activation. EMBO J. *27*, 373–383.
16. Bhoj, V.G., and Chen, Z.J. (2009). Ubiquitylation in innate and adaptive immunity. Nature *458*, 430–437.
17. Hustad, C.M., Perry, W.L., Siracusa, L.D., Rasberry, C., Cobb, L., et al. (1995). Molecular genetic characterization of six recessive viable alleles of the mouse agouti locus. Genetics *140*, 255–265.
18. Perry, W.L., Hustad, C.M., Swing, D.A., O'Sullivan, T.N., Jenkins, N.A., and Copeland, N.G. (1998). The *itchy* locus encodes a novel ubiquitin protein ligase that is disrupted in a18H mice. Nat. Genet. *18*, 143–146.
19. Angers, A., Ramjaun, A.R., and McPherson, P.S. (2004). The HECT domain ligase itch ubiquitinates endophilin and localizes to the trans-Golgi network and endosomal system. J. Biol. Chem. *279*, 11471–11479.
20. Matesic, L.E., Copeland, N.G., and Jenkins, N.A. (2008). *Itchy* mice: the identification of a new pathway for the development of autoimmunity. Curr. Top. Microbiol. Immunol. *321*, 185–200.
21. Shembade, N., Harhaj, N.S., Parvatiyar, K., Copeland, N.G., Jenkins, N.A., Matesic, L.E., and Harhaj, E.W. (2008). The E3 ligase Itch negatively

regulates inflammatory signaling pathways by controlling the function of the ubiquitin-editing enzyme A20. Nat. Immunol. *9*, 254–262.

22. Song, H.Y., Régnier, C.H., Kirschning, C.J., Goeddel, D.V., and Rothe, M. (1997). Tumor necrosis factor (TNF)-mediated kinase cascades: bifurcation of nuclear factor-kappaB and c-jun N-terminal kinase (JNK/SAPK) pathways at TNF receptor-associated factor 2. Proc. Natl. Acad. Sci. USA *94*, 9792–9796.
23. Häcker, H., Redecke, V., Blagoev, B., Kratchmarova, I., Hsu, L.C., Wang, G.G., Kamps, M.P., Raz, E., Wagner, H., Häcker, G., et al. (2006). Specificity in Toll-like receptor signalling through distinct effector functions of TRAF3 and TRAF6. Nature *439*, 204–207.
24. Oganesyan, G., Saha, S.K., Guo, B., He, J.Q., Shahangian, A., Zarnegar, B., Perry, A., and Cheng, G. (2006). Critical role of TRAF3 in the Toll-like receptor-dependent and -independent antiviral response. Nature *439*, 208–211.
25. Takeshita, F., Ishii, K.J., Kobiyama, K., Kojima, Y., Coban, C., Sasaki, S., Ishii, N., Klinman, D.M., Okuda, K., Akira, S., and Suzuki, K. (2005). TRAF4 acts as a silencer in TLR-mediated signaling through the association with TRAF6 and TRIF. Eur. J. Immunol. *35*, 2477–2485.
26. Chastagner, P., Israël, A., and Brou, C. (2006). Itch/AIP4 mediates Deltex degradation through the formation of K29-linked polyubiquitin chains. EMBO Rep. *7*, 1147–1153.
27. Scialpi, F., Malatesta, M., Peschiaroli, A., Rossi, M., Melino, G., and Bernassola, F. (2008). Itch self-polyubiquitylation occurs through lysine-63 linkages. Biochem. Pharmacol. *76*, 1515–1521.
28. Wertz, I.E., O'Rourke, K.M., Zhou, H., Eby, M., Aravind, L., Seshagiri, S., Wu, P., Wiesmann, C., Baker, R., Boone, D.L., et al. (2004). De-ubiquitination and ubiquitin ligase domains of A20 downregulate NF-kappaB signalling. Nature *430*, 694–699.
29. Hitotsumatsu, O., Ahmad, R.C., Tavares, R., Wang, M., Philpott, D., Turer, E.E., Lee, B.L., Shiffin, N., Advincula, R., Malynn, B.A., et al. (2008). The ubiquitin-editing enzyme A20 restricts nucleotide-binding oligomerization domain containing 2-triggered signals. Immunity *28*, 381–390.
30. Hutti, J.E., Turk, B.E., Asara, J.M., Ma, A., Cantley, L.C., and Abbott, D.W. (2007). IkappaB kinase beta phosphorylates the K63 deubiquitinase A20 to cause feedback inhibition of the NF-kappaB pathway. Mol. Cell. Biol. *27*, 7451–7461.
31. Kim, Y.G., Park, J.H., Shaw, M.H., Franchi, L., Inohara, N., and Núñez, G. (2008). The cytosolic sensors Nod1 and Nod2 are critical for bacterial recognition and host defense after exposure to Toll-like receptor ligands. Immunity *28*, 246–257.
32. Herskovits, A.A., Auerbuch, V., and Portnoy, D.A. (2007). Bacterial ligands generated in a phagosome are targets of the cytosolic innate immune system. PLoS Pathog. *3*, e51.
33. Leber, J.H., Crimmins, G.T., Raghavan, S., Meyer-Morse, N.P., Cox, J.S., and Portnoy, D.A. (2008). Distinct TLR- and NLR-mediated transcriptional responses to an intracellular pathogen. PLoS Pathog. *4*, e6.
34. Gutierrez, O., Pipaon, C., Inohara, N., Fontalba, A., Ogura, Y., Prosper, F., Nunez, G., and Fernandez-Luna, J.L. (2002). Induction of Nod2 in myelomonocytic and intestinal epithelial cells via nuclear factor-kappa B activation. J. Biol. Chem. *277*, 41701–41705.
35. Bertrand, M.J., Doiron, K., Labbé, K., Korneluk, R.G., Barker, P.A., and Saleh, M. (2009). Cellular Inhibitors of Apoptosis cIAP1 and cIAP2 Are Required for Innate Immunity Signaling by the Pattern Recognition Receptors NOD1 and NOD2 (Immunity) ([Epub May 20 ahead of print]).
36. Inohara, N., Koseki, T., del Peso, L., Hu, Y., Yee, C., et al. (1999). Nod1, an Apaf-1-like activator of caspase-9 and nuclear factor-kB. J. Biol. Chem. *274*, 14560–14567.
37. Clark, N.M., Marinis, J.M., Cobb, B.A., and Abbott, D.W. (2008). MEKK4 sequesters RIP2 to dictate NOD2 signal specificity. Curr. Biol. *18*, 1402–1408.
38. Marina-García, N., Franchi, L., Kim, Y.G., Miller, D., McDonald, C., Boons, G.J., and Núñez, G. (2008). Pannexin-1-mediated intracellular delivery of muramyl dipeptide induces caspase-1 activation via cryopyrin/NLRP3 independently of Nod2. J. Immunol. *180*, 4050–4057.
39. Du, P., Kibbe, W.A., and Lin, S.M. (2008). lumi: a pipeline for processing Illumina microarray. Bioinformatics *24*, 1547–1548.
40. Eisen, M.B., Spellman, P.T., Brown, P.O., and Botstein, D. (1998). Cluster analysis and display of genome-wide expression patterns. Proc. Natl. Acad. Sci. USA *95*, 14863–14868.